Composites: Part A 39 (2008) 1547–1555

Contents lists available at ScienceDirect

Composites: Part A

journal homepage: www.elsevier.com/locate/compositesa

Prediction of the adhesive fillet size for skin to honeycomb core bonding in ultra-light sandwich structures

Julien Rion, Yves Leterrier, Jan-Anders E. Månson *

Laboratoire de Technologie des Composites et Polymères (LTC), Ecole Polytechnique Fédérale de Lausanne (EPFL), CH-1015 Lausanne, Switzerland

ARTICLE INFO

Article history:
Received 2 October 2007
Received in revised form 30 May 2008
Accepted 30 May 2008

Keywords:
A: Honeycomb
B: Debonding
Adhesive meniscus

ABSTRACT

The formation of resin fillet between honeycomb core cell walls and skin in light sandwich structures was studied to gain a better understanding of the bonding process. A method was developed for tailoring the amount of adhesive between 8 and 80 g/m^2. The size of the adhesive menisci and the contact angles between the adhesive and the skin and the core materials were measured. A model was developed to predict the size of the menisci. Their shape was driven by the surface energy of skin and honeycomb materials. When adhesive films were used for bonding, up to 50% of the adhesive did not form the menisci whereas 100% did when the newly developed adhesive deposition method on honeycomb was used, which allowed better bonding with lower weight.

1. Introduction

Composite sandwich structures are increasingly used in applications requiring high strength and stiffness-to-weight ratio. These properties allow improved performance and reduction in weight, and are therefore of great interest in aeronautical applications [1–4], and in all applications where weight saving is a priority. The sandwich structures comprise skins adhesively bonded to a core. The skins are thin sheets of metal or composite of high strength and stiffness. The core is made of lightweight material such as balsa, foam or honeycomb. To design an optimal structure, i.e. with the highest strength-to-weight ratio, all failure modes of each constituent have to be considered. In fact, in the ideal structure, all failure modes should occur simultaneously [5,6]. The elements which do not fail at the ultimate load level of the structure are over-designed, and thus their dimensions and weight can be reduced without decreasing the failure load of the structure. Therefore, the optimal design of the structure requires precise knowledge of the strength of the different constituents.

Energy saving by weight reduction is of primary importance for very high-tech applications such as ultra-light solar cars, ultra-light airplanes or satellites. In those applications the use of ultra-light sandwich structures is often the best solution to achieve a minimum weight design. The weight of these structures can be less than 1 kg/m^2, which is extremely low in comparison with the usual sandwich construction for commercial airplanes or marine applications. Therefore, sandwich structures with thin facings and very low-density honeycomb cores are preferred.

For the design of such ultra-light sandwich structures weighing less than 1 kg/m^2, the criteria and methods used for traditional sandwich structures are not sufficient to ensure an optimal strength-to-weight ratio. The classic considerations governing core and skin strength as described in [7–9] can be used for a first predesign. However, in sandwich structures with thin skins, the dominant failure mode is often local instability of the skin in compression. The skin can either buckle into the core or debond from the core. The first case has been extensively studied and a summary of the most often used models is proposed in [10]. An improved model of the intra-cell buckling of the skin in the case of a honeycomb core was proposed by Thomsen and Banks [11] and was shown to provide more accurate predictions than the classic design formulae. Fagerberg and Zenkert [12] described a model which took into account the initial imperfection of the skins, thus enabling improved prediction of the wrinkling stress of the skin.

The failure of the structure due to core-skin debonding has also been studied by numerous authors. The test methods described in the ASTM standards [13–15], as well as many variations and adaptations [16–20] have often been used to measure the core/skin debonding energy on sandwich panels using various core and skin materials. However, only a few studies have investigated the microscopic fracture mechanisms that occur during honeycomb core-skin debonding in sandwich panels. Okada and Kortschot [21] studied the importance of the resin fillet during core/skin delamination. They showed that a bigger resin fillet absorbs more energy during delamination, due to energy dissipation phenomena. In fact, because of the energy dissipation in the resin fillets, the

* Corresponding author. Tel.: +41 21 693 42 81; fax: +41 21 693 58 80.
E-mail address: jan-anders.manson@epfl.ch (Jan-Anders E. Månson).

1359-835X/$ - see front matter © 2008 Elsevier Ltd. All rights reserved.
doi:10.1016/j.compositesa.2008.05.022

strain energy release-rate value of the honeycomb core-to-skin bonding can exceed that of a laminate made from the skin material, even though the area of resin fractured is lower. Grove et al. [22] showed that the higher debonding energy was obtained with larger, regular-shaped adhesive fillets between the honeycomb cell walls and the skin. The same claim was made by Allegri et al. [23] who obtained the best bonding with their automated process ensuring the formation of a regular-shaped meniscus. Rion et al. [24] showed that failure occurs in the adhesive meniscus when low adhesive weight is used, and so further demonstrated the necessity of forming a regular-shaped adhesive meniscus. They also observed that debonding energy of the skin measured with climbing drum peel test increased with meniscus size until the failure occurred in the honeycomb core, and not anymore in the menisci. Hayes et al. [25] showed that not only the size, but also the quality of the resin fillet plays a role. They made a sandwich with a commercial self-adhesive prepreg and a home-made model prepreg with less solvent content. They showed that the solvent leads to porosity formation and then to a decrease in debonding energy.

Chanteranne [26] studied the influence of the honeycomb cell size on meniscus size. He found that the height of the fillets increased with the size of the honeycomb cells due to the larger amount of adhesive available, and that the associated debonding energy was higher. He also observed that the humidity level in the processing room and a primer treatment of the aluminium honeycomb can greatly influence meniscus height, and thus debonding strength, the greatest strength being associated with high menisci.

These different studies demonstrate the considerable influence of the microscopic failure process on the debonding energy. To understand these mechanisms, it is vital to know precisely the size and the shape of the meniscus. Furthermore, to be able to predict the debonding energy, the size and shape of the menisci have to be predicted. Therefore, the aim of this study was to develop a model allowing accurate prediction of the fillet size as a function of the properties of the different sandwich constituents. The model was tested using various adhesive quantities for core-to-skin bonding. To this end a method was developed allowing a choice of the amount of adhesive used for bonding the skin to the honeycomb core. This method and the model are a first step for the understanding of bonding mechanisms between honeycomb core and skin and will be useful for a subsequent optimization of the adhesive weight and process, i.e. for defining parameters giving highest strength to weight ratio.

2. Materials and methods

2.1. Materials and sandwich processing

The ultra-light sandwich structures studied were made of carbon fiber prepreg skins and honeycomb cores. The skins were fabricated with UD carbon-fiber prepregs with 66 wt% carbon fibers (200 g/m^2 T700 fibers from Toray), and an epoxy matrix (Advanced Composite Group (ACG) VTM 264). Carbon fibers were chosen because they offer the best strength and stiffness-to-weight ratio. The use of prepregs ensures a high fiber-to-resin fraction and enables the quantity of resin in the skin to be controlled accurately, thereby achieving high quality and good reproducibility, which are of primary importance in designing structural parts. The use of prepregs is also very convenient for composite manufacturing since it avoids the need to use liquid resin. However, the disadvantages of the prepregs are their limited drapability, limited lifetime, and their higher price.

The core was a 29 kg/m^3 Nomex® honeycomb of aerospace grade (Euro-Composite® ECA) with a 3.2 mm cell diameter and 8 mm thickness. Nomex® is an Aramid fiber paper dipped in phenolic resin. A thermosetting adhesive is used to bond the Nomex® sheets at the nodes and, after expanding to the hexagonal configuration, the core is dipped in phenolic resin to keep the shape. Honeycomb is known to be the core material offering the best stiffness and strength-to-weight ratio and is therefore widely used in the aerospace industry as well as in all domains requiring high specific mechanical properties. Nomex® honeycomb core is easily available at low density and was therefore chosen as core material.

The adhesive used for skin-to-core bonding was rubber-toughened epoxy resin (VTA 260 adhesive film from ACG), either 50, 150 or 300 g/m^2, which offers good bonding capability on composite substrates and aluminium.

As a first step, and in order to control exactly the amount of glue in the resin menisci forming between the skins and the honeycomb cell walls, the skins were cured separately under vacuum on an aluminium plate, so that the prepreg resin did not participate in the bonding process. The vacuum applied created a relative pressure of −0.9 bar under the vacuum bag. The skin was cured at 120 °C for 70 min and the heating rate was 1 °C/min. During this process, a peel-ply was placed on the skin to create surface roughness in order to improve subsequent bonding with the core (Fig. 1) [27]. It is essential to use a peel-ply which does not transfer any silicone or fluorinated elements onto the prepreg surface, otherwise the adhesion will be reduced dramatically. The peel-ply used in this study was A100 PS from Aerovac, a nylon fabric producing a medium texture. It has been observed that by using Silicone (Airtech Bleeder Lease B) and Teflon (Airtech Release Ease 234 TF NP)-coated peel-plies the skin peeling energy was reduced by 55% respectively 98% compared to the peel-ply used in this study.

The amount of adhesive for skin-to-core bonding was controlled using the following method (Fig. 2). A paper coated with a thin layer of heat-curable epoxy was placed onto the honeycomb and maintained under slight pressure by means of a steel block. The assembly was subsequently put in a temperature-controlled oven (at 45, 50, 55, 60 or 70 °C) for a few minutes (0.5–15 min), long enough to allow a drop in resin viscosity, but short enough to avoid the polymerization of the resin system. The paper was then removed immediately after taking the plate out of the oven, leaving an adhesive quantity on the honeycomb directly dependent on the time and temperature in the oven. This method was tested with 150 and 300 g/m^2 VTA 260 adhesive films from ACG and also with 86 g/m^2 EH84 resin system from Hexcel.

The honeycomb with the controlled amount of glue was finally placed on the cured carbon skin on an aluminium plate, and the panel was cured under vacuum at 120 °C for 70 min following a heating ramp of 1 °C/min. The same process was used for bonding the second skin.

Cross-sections of the sandwich panels were then prepared in order to investigate the morphology of the adhesive meniscus. Sam-

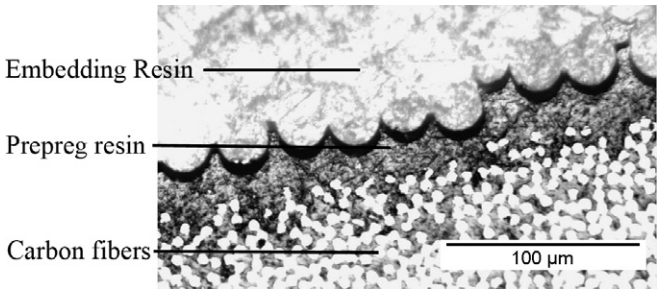

Fig. 1. Cross-section of carbon-fiber skin after peel-ply removal. The surface texture enables improved subsequent bonding, an increase in adhesive surface, and creates mechanical anchoring of the resin.

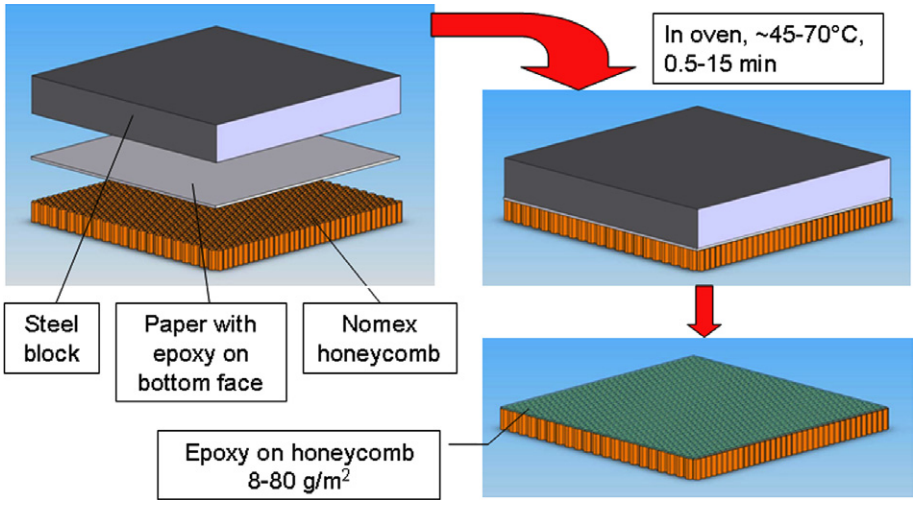

Fig. 2. Adhesive deposition method. The steel block was used to press the adhesive onto the honeycomb. After removing the paper, a thin and controlled adhesive layer stayed on the honeycomb.

ples were cut from the panels, and the honeycomb was cut between the two skins, so that the cells could be filled with embedding resin. The embedded samples were polished with SiC paper of grades 220, 500, 1000, 2400 and finally 4000 and the size of the meniscus was measured using optical microscopy. The depth of polishing was carefully controlled, so that the cross-section was in a zone perpendicular to the hexagonal cell wall. The shape and size of the meniscus between skin and cell wall could therefore be measured without need of correction factor due to misalignment problem.

2.2. Apparent contact angle measurements

The shape of the resin fillet is essentially a function of the contact angles of the adhesive on the skin and core material. The contact angles were measured on the cured prepreg surface (after removal of the peel-ply), and on the honeycomb cell walls using the sessile drop technique [28–30]. In the latter case, bands of Nomex were peeled from the honeycomb panel and fixed onto a plate in order to have a flat surface.

Small pieces of adhesive film were cut and deposited on the carbon or Nomex surface, and cured either at 80 or at 120 °C in order to observe the effect of the processing temperature. Shrinkage of the resin during curing may slightly change the shape of the drop, and so the contact angles measured in the solid state are not the real contact angles of the resin, but apparent contact angles. Furthermore, the pronounced roughness of the surfaces, especially the prepreg surface after peel-ply removal, has a significant influence on the contact angle. Indeed the free energy of the surface is increased as a result of the increase of the effective surface and thus changes the contact angle. The theory of Wenzel enables the real contact angle on a smooth surface to be calculated, based on the contact angle measured on the rough surface and a roughness parameter [31–33]. This shows that the contact angle will be decreased on a rough surface when the liquid wets the surface, and will be increased when the angle is larger than 90°. The improved wetting of the prepreg surface treated with peel-ply has been highlighted by Benard et al. [34] and it is particularly interesting to have good adhesion on the surface. The contact angle measured in the present study is the apparent contact angle on the rough surface. As the modeling of the meniscus formation only requires the contact angles with the real rough surface, the corresponding true contact angle on a smooth surface was not calculated.

A significant contact angle hysteresis was observed, and the advancing and receding angles were measured. This effect is usually attributed to surface roughness and heterogeneities [28]. For the advancing angle, small balls of adhesive were laid on the surface and then spread spontaneously over the surface during curing. For the receding angle, small pieces of 50 μm thick adhesive film were laid on the surface and these retracted due to surface tension during curing to form sessile drops.

The size of the drop is limited by gravity effects. The influence of gravity on the shape of the drop is characterized by the Bond number [28]

$$B = \frac{gR^2\Delta\rho}{\gamma} \tag{1}$$

where g is the acceleration due to gravity, $\Delta\rho$ the difference of density between the air and the liquid forming the drop, R is the radius of a sphere with the same volume as the sessile drop, and γ is the surface tension of the liquid. When the Bond number is zero, the drop is a truncated sphere. To estimate the Bond number in the present case, and as the surface tension of the adhesive is not known, values of surface tension of an epoxy resin system (Ciba, LY 5082) as measured by Page et al. [35] using the Wilhelmy slide method [28,30] were used. They ascertained a surface tension of about 35 mJ/m^2 for the uncured resin at room temperature. They showed that surface tension decreases slightly when temperature increases (33.6 mJ/m^2 at 80 °C), and increases with the rate of conversion during curing (~43 mJ/m^2 fully cured at 80 °C). However, the change of the Bond number due to these variations is negligible.

Considering g = 9.81 m/s^2, the difference between resin density and air $\Delta\rho$ = 1189 kg/m^3 and R = 0.4 mm which corresponds to the drops considered in the measurements, the Bond number is 0.05. According to the work of Smith and Van De Ven [36], using this Bond number, associated with the small value of the contact angles measured, the error in angle measurement due to gravity (considering that the drop has a spherical shape) is less than 0.5°, which is smaller than the standard deviation of the measurements.

As the viscosity of the adhesive is a function of the temperature, the drops were cured either at 80 or at 120 °C in order to determine the influence of the temperature on the contact angle. Curing was carried out at atmospheric pressure as well as under vacuum.

After curing, the drops were cross-cut and polished to the center with SiC paper of grade 1000. The advance of the polishing was

controlled with an optical microscope in order to stop polishing at the center of the drop. The drop diameter was measured prior to polishing using the microscope and the polishing was stopped when half of the drop diameter was removed. The height h of the drop and the diameter L of the contact line circle (see Section 4) were measured under microscope in order to calculate the contact angle θ:

$$\tan\left(\frac{\theta}{2}\right) = \frac{2h}{L} \tag{2}$$

3. Fillet shape modeling

The resin fillets are 3D structures with hexagonal symmetry. Their cross-section is, however, independent of position along most of the honeycomb cell wall, with only a small change in the corner of the hexagonal cell. Therefore, to predict the shape of the resin fillet, a 2D model was designed with two perpendicular planes and a resin fillet (Fig. 3). The two contact angles θ_1 and θ_2 were defined by the different surface tensions, and the area under the meniscus A was fixed by the volume of adhesive, considered to be incompressible.

By using the Young–Laplace equation [28]

$$\Delta P = \gamma_{lv}\left(\frac{1}{R_1} + \frac{1}{R_2}\right) \tag{3}$$

where R_1 and R_2 are the two radii of curvature of the meniscus surface, γ_{lv} the surface tension of the adhesive at liquid vapor interface, ΔP is the pressure difference between the inside and outside of the meniscus, and, considering that for the 2D case R_2 is infinite, we have

$$\Delta P = \frac{\gamma_{lv}}{R} \tag{4}$$

If the effect of gravity is disregarded, ΔP is constant and thus R is also constant [37]. The free surface of the meniscus is circular with radius and center determined by the contact angles and the area of the meniscus.

This result was also obtained by considering equilibrium equations, as represented in Fig. 3:

$$\gamma_{lv}\,\mathrm{d}\theta \cong \Delta P\,\mathrm{d}l \tag{5}$$

with

$$\mathrm{d}l = \sqrt{\mathrm{d}x^2 + \mathrm{d}y^2} = \mathrm{d}x\sqrt{1 + \left(\frac{\mathrm{d}y}{\mathrm{d}x}\right)^2} = \mathrm{d}x\sqrt{1 + y\prime(x)^2} \tag{6}$$

As

$$\theta = \arctan(y'(x)) \tag{7}$$

we have

$$\frac{\mathrm{d}\theta}{\mathrm{d}x} = \frac{y''(x)}{1 + y'(x)^2} \tag{8}$$

and thus

$$\frac{\mathrm{d}\theta}{\mathrm{d}l} = \frac{\mathrm{d}\theta}{\mathrm{d}x}\frac{\mathrm{d}x}{\mathrm{d}l} = \frac{y''(x)}{(1 + y'(x)^2)\sqrt{1 + y'(x)^2}} = \frac{y''(x)}{(1 + y'(x)^2)^{3/2}} \cong \frac{\Delta P}{\gamma_{lv}} \tag{9}$$

By introducing in (9) a circle equation of center $(X_c; Y_c)$ and radius R

$$y(x) = Y_c - \sqrt{R^2 - x^2 + 2xX_c - X_c^2} \tag{10}$$

we obtain

$$\frac{\Delta P}{\gamma_{lv}} = \frac{1}{R} \tag{11}$$

which is exactly the Young–Laplace equation for the 2D case.

The center of the circle can easily be determined as

$$\begin{aligned} X_c &= R\cos(\theta_1) \\ Y_c &= R\cos(\theta_2) \end{aligned} \tag{12}$$

The fillet should thus have a concave shape if the contact angles are smaller than 90°, i.e. if the adhesive wets the surfaces. The radius of the circle is determined by the area of the resin fillet (Fig. 4) using following equations:

$$\begin{aligned} L_1 &= R\cos(\theta_2) - R\sin(\theta_1) \\ L_2 &= R\cos(\theta_1) - R\sin(\theta_2) \end{aligned} \tag{13}$$

and

$$A = \frac{L_2 R\cos(\theta_2) + L_1 R\cos(\theta_1) - R^2\left(\frac{\pi}{2} - \theta_1 - \theta_2\right)}{2} \tag{14}$$

However, the area of the meniscus depends of the quantity of adhesive available for its formation. This was well-controlled when the adhesive forming the meniscus was directly put onto the honeycomb, as described in Fig. 2, and the skin was already cured, but

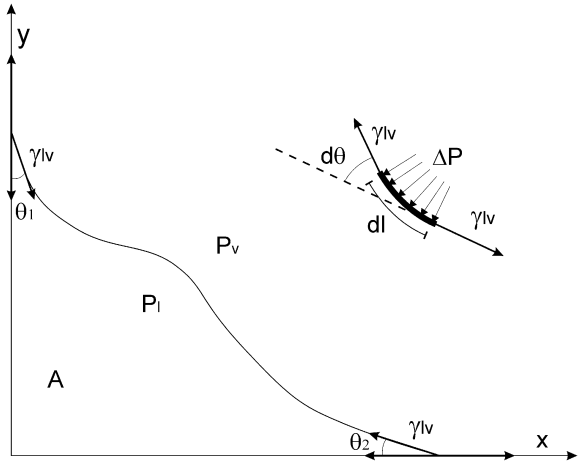

Fig. 3. Calculation of the shape of the meniscus. The contact angles are determined by the surface tension, and the area A is fixed by the fillet volume. The forces involved in achieving equilibrium are the surface tension and the pressure difference.

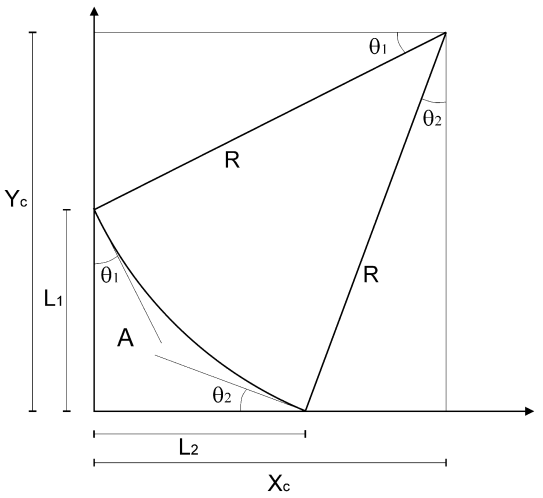

Fig. 4. Fillet with constant radius of curvature. The radius R is determined by the area of the fillet.

in cases where adhesive film, or one-shot processing were used, the amount of resin from the adhesive film and from the prepreg forming the meniscus was unknown and depended on the processing conditions, i.e. mainly the temperature and the level of vacuum applied.

The relation between the height of the meniscus L_1 and the weight per unit area of adhesive could be easily calculated for honeycomb with hexagonal cells working on the hypothesis that the 2D model is valid in the entire honeycomb cell. Actually, in the cell corners between two adjacent cell walls, the meniscus presents a double curvature which changes the geometry. Nevertheless, in case of small menisci ($L_2/d \sim 0.1$), the deviation is only located in the cell corners and the 2D model is valid on the largest part of the cells. By assuming a triangular meniscus of height L_1 and width L_2, the volume of adhesive contained in one hexagonal cell is

$$V = 6\left(\frac{dL_1L_2}{4} - \frac{L_1L_2^2\tan(\pi/6)}{3}\right) \tag{15}$$

where d is the outer diameter of the honeycomb cell, i.e. the distance between two opposite corners of the hexagonal cells. As the surface of one honeycomb cell is

$$S = \frac{3\sqrt{3}d^2}{8} \tag{16}$$

the adhesive areal weight depends on the size of the fillet according to:

$$M = \alpha\left(\frac{4L_1L_2}{\sqrt{3}d} - \frac{16L_1\tan(\pi/6)L_2^2}{3\sqrt{3}d^2}\right)\rho \tag{17}$$

where ρ is the density of the adhesive and α the ratio between the real meniscus and the triangular shape approximation (Fig. 5), given by

$$\alpha = \frac{2A}{L_1L_2} = \frac{L_2R\cos(\theta_2) + L_1R\cos(\theta_1) - R^2\left(\frac{\pi}{2} - \theta_1 - \theta_2\right)}{L_1L_2} \tag{18}$$

Knowing the contact angles of the adhesive with the skin and honeycomb, the shape and size of the meniscus could then be predicted with Eqs. (13)–(18).

In the Young–Laplace equation (4), if the meniscus forms with a concave shape (Fig. 4), R is positive and thus ΔP is positive. This means that the pressure in the meniscus is lower than the ambient pressure. This explains why the resin flowed in the meniscus. If the radius is convex, ΔP is negative and the meniscus can not form. Furthermore, ΔP decreases when R increases. As the system will automatically tend to equilibrium, the radius tends to be as big as possible, as a function of the adhesive available, and as long as gravity can be disregarded. So when equilibrium is reached, the quantity of adhesive in the meniscus is only determined by the amount of adhesive in contact with the meniscus, and the geometry by the contact angles. If highly viscous adhesive is used, polymerization may occur before equilibrium is reached, i.e. before the adhesive has completely flown in the meniscus. In this case, the size of the meniscus will also be controlled by the temperature-dependent chemo-rheological properties of the adhesive. These complex transient phenomena could be disregarded in the present study since resin viscosity was rather low at the selected curing temperature.

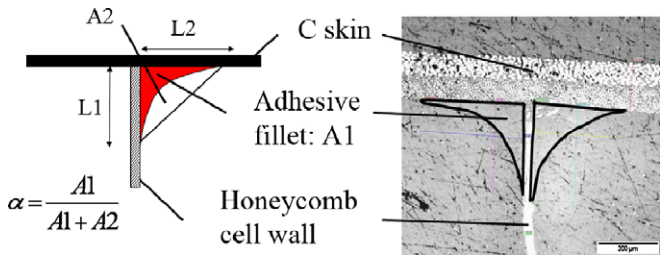

Fig. 5. Fillet shape, triangular approximation, and ratio α determining the real shape.

4. Results and discussion

4.1. Adhesive deposition method

By varying time and temperature in the oven, an adhesive weight ranging from 8 to 80 g/m^2 was obtained on honeycomb as depicted in Figs. 6 and 7. The type and viscosity of the adhesive, as well as the type of transfer paper on the film were crucial factors determining the quantity of adhesive transferring onto honeycomb. These results allow an accurate choice to be made concerning the quantity of adhesive required for skin-to-core bonding; this is of great interest in studying resin meniscus shape as a function of adhesive weight. This method is not limited to the specific core and adhesives used in this study, and can be adapted to any other adhesive presenting viscosity drop with temperature. The temperature in oven should be high enough to allow viscosity drop and the time should be short in comparison to the curing time to avoid reticulation of the resin. As a guideline, the temperature used should be close to the curing temperature of the adhesive when it is cured in about 10 h.

Another advantage of this method is that the adhesive is laid directly on top of the cell walls where the resin fillets form during bonding. No excess adhesive is used, (i.e. there is none in the center of honeycomb cells), thereby allowing weight saving without decreasing bonding capability. This method is therefore well suited and accurate to produce ultra-light sandwich panels, and is easily adaptable to automatically deposit adhesive on large panels. One can imagine for example passing the honeycomb panel through two heated rolls pressing the adhesive films on both faces of honeycomb and peeling them after the rolls. By adjusting the pressing load, temperature and speed of the rolls, the adhesive quantity could be chosen.

As all the resin is in the resin fillet between cell walls and the skin, it is then possible, by using the model described above, to predict the geometry and size of the resin fillet based on the adhesive weight.

4.2. Fillet size prediction and measurements

The apparent contact angle of the adhesive deposited on the prepreg and Nomex was calculated from the width and height of

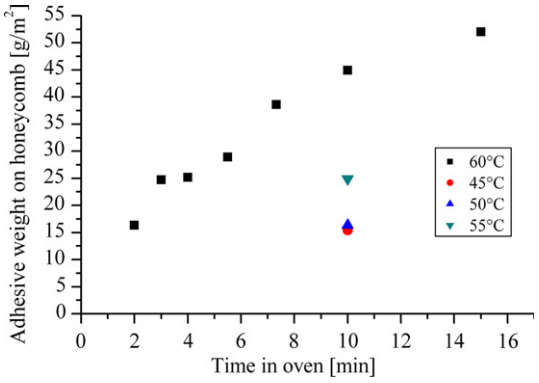

Fig. 6. Adhesive weight laid on honeycomb with 86 g/m^2 EH84 adhesive film.

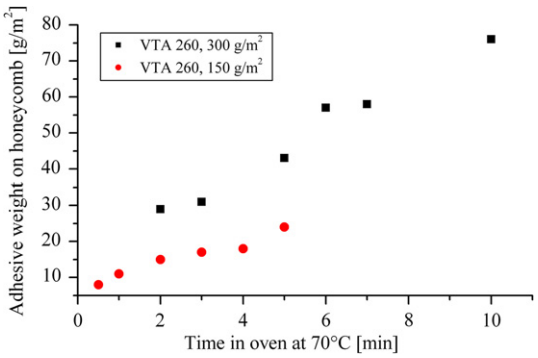

Fig. 7. Adhesive weight laid on honeycomb with ACG adhesive films.

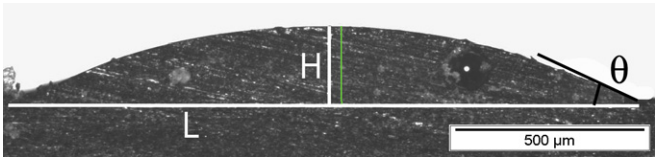

Fig. 8. Adhesive sessile drop on carbon prepreg. The adhesive was cured at 80°. The height H, diameter L and contact angle θ are represented.

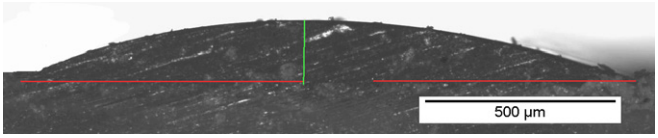

Fig. 9. Adhesive sessile drop on Nomex honeycomb. The adhesive was cured at 80°.

the drops. Due to the roughness of the honeycomb surface and of the carbon prepreg after peel-ply removal, the adhesive drops did not systematically adopt a regular sessile drop shape. When vacuum was applied, bubbles occasionally formed in the drop and then changed its form. In calculating the contact angle, only the drops with a regular shape were considered (Figs. 8 and 9). The contact angles measured are represented in Table 1. The advancing angles were smaller when the adhesive was cured at 120 °C rather than at 80 °C. This was due to the lower viscosity of the adhesive at 120 °C, enabling the resin to spread more easily than it did at 80 °C. The effect of resin viscosity was confirmed by the fact that the difference between advancing and receding angles was more pronounced at 80 °C than at 120 °C.

The receding angles changed only slightly under the different curing conditions. Actually, the pieces of adhesive film laid on the surface did not really retract to form sessile drops, due to the high viscosity of the adhesive, and this caused errors in the measurements. The receding angles were too small to be measured accurately with this method. However, the angles measured could be considered as being at the upper limit of the real receding angles which would form if the resin was less viscous and if the equilibrium state was reached during curing.

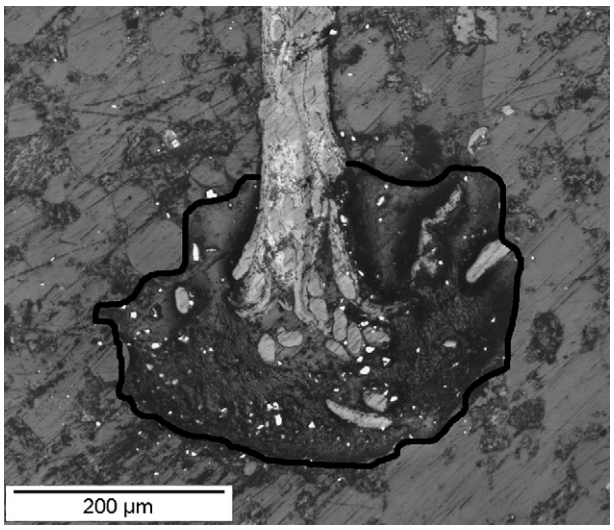

Fig. 10. Adhesive on the top of a honeycomb cell wall after deposition of 22 g/m^2 adhesive. Adhesive surface has been highlighted with black line for better visibility.

The advancing contact angles measured when the adhesive was cured under vacuum were slightly lower than those under atmospheric pressure, but the difference was smaller than the standard deviation and was thus not significant.

The shape factor of the meniscus was then calculated with Eq. (18). The weight per unit area of adhesive as a function of the contact angles and height of meniscus could be determined with Eq. (17).

4.2.1. Meniscus size with adhesive deposition method

When the adhesive deposition method is used, the adhesive stays at the top of the honeycomb cell wall (Fig. 10). During skin bonding, the adhesive has to spread onto the carbon surface as well as onto the honeycomb surface. Therefore, the advancing angles for both surfaces have to be taken into account in predicting fillet size. The predicted fillet size in these conditions as a function of adhesive weight is represented in Fig. 11 with the height of resin fillet measured on sandwich samples produced with various adhesive quantities. The changing size and shape of the meniscus is illustrated in Fig. 12 and confirms its predicted circular shape, especially in the case of a large meniscus. However the adhesive menisci sometimes have an irregular shape due to the rough surface of the Nomex and prepreg. In fact, small Aramid fibers pointing out of the honeycomb cell wall surface can completely change the meniscus shape, and thus the height of the meniscus differs from the one with a circular shape (Fig. 13). These irregularities explain the large standard deviation of the measurements.

Table 1
Contact angles measured with adhesive VTA 260 on carbon prepreg and Nomex honeycomb, with adhesive cured at 80° or 120° either under vacuum or at ambient pressure

	Carbon prepreg: mean angle [°]	SD	Nomex honeycomb: mean angle [°]	SD
80 °C advancing angle	24.0	3.5	23.1	4.9
80 °C receding angle	8.9	2.2	6.3	2.0
120 °C advancing angle	15.3	2.3	16.6	1.0
120 °C receding angle	8.5	2.6	9.4	0.5
120 °C advancing angle with vacuum	12.5	1.9	13.9	3.3
120 °C receding angle with vacuum	7.7	2.7	11.1	5.7

The mean value and standard deviation of 10 measurements is indicated for each case.

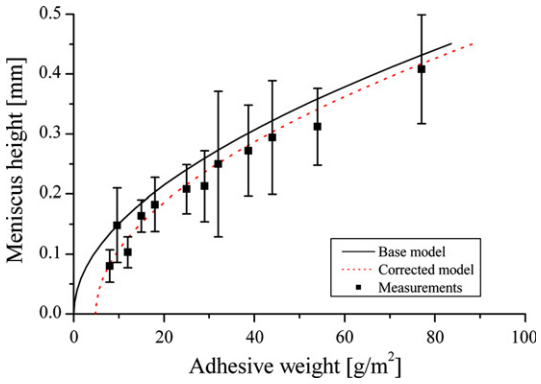

Fig. 11. Meniscus height predicted as a function of adhesive weight and contact angles. The contact angle with the carbon was measured as 13° and with the Nomex as 14°. The corresponding shape factor is $\alpha = 0.60$. For the corrected model, the adhesive weight M_0, which is not in the meniscus, was calculated to be 4.85 g/m^2.

When comparing the predictions to the actual measurements, it is noticeable that the average size of the meniscus is overestimated by the model (Fig. 11). In fact the model considers that all the resin is used to form a meniscus between two perfectly smooth surfaces. Actually, as the prepreg and the Nomex are rough, some resin remains between the prepreg and the honeycomb cell wall, instead of forming the meniscus (Fig. 14). This is accounted for with the following modification of Eq. (17):

$$M = \alpha\left(\frac{4L_1L_2}{\sqrt{3}d} - \frac{16L_1\tan(\pi/6)L_2^2}{3\sqrt{3}d^2}\right)\rho + M_0 \tag{19}$$

where M_0 is the weight per unit area of adhesive not involved in forming the meniscus. The value M_0 minimizing the difference between the measured height and the predicted height with the least squares method is 4.85 g/m^2. Allowing for this correction, the model describes very well the average size of the meniscus. This model can thus be used for any combination of core, skin and adhesive materials, providing the contact angle of the adhesive on the core and skin materials is known at the curing temperature. The value of M_0 has to be adapted according to the roughness of the cured skin.

Furthermore, with the known meniscus size, the assumption that gravity can be disregarded in calculating meniscus shape can be verified. By considering a fillet radius of 0.5 mm, and with the epoxy surface tension according to Page et al. [35], the Young–Laplace equation (11) gives $\Delta P = 70$ Pa. In comparison, the pressure exerted by gravity with a 0.5 mm epoxy column is

$$\rho g h = 1190 \times 9.81 \times 0.5 = 5.8 \text{ Pa} \tag{20}$$

which is small in comparison, and further confirms the hypothesis of discounting gravity.

4.2.2. Meniscus size with commercial adhesive films

When continuous commercial adhesive films were used for skin-to-core bonding, it was assumed that the contact angle with the prepreg is 0°, as the film completely covered the surface. On the honeycomb, the advancing angle should be considered as for the preceding case. However in the present case a large amount of adhesive remained at the surface of the prepreg in the honeycomb cell instead of forming the meniscus. This was mainly due to the high roughness of the carbon prepreg surface after removing the peel-ply. The mean thickness of the adhesive left on the surface was measured on micrographs. As the surface was very rough, a mean thickness was calculated on each micrograph as shown in Fig. 15. The mean thickness measured was 21 μm, which corresponds to 25 g/m^2 adhesive. The amount of resin, which was not

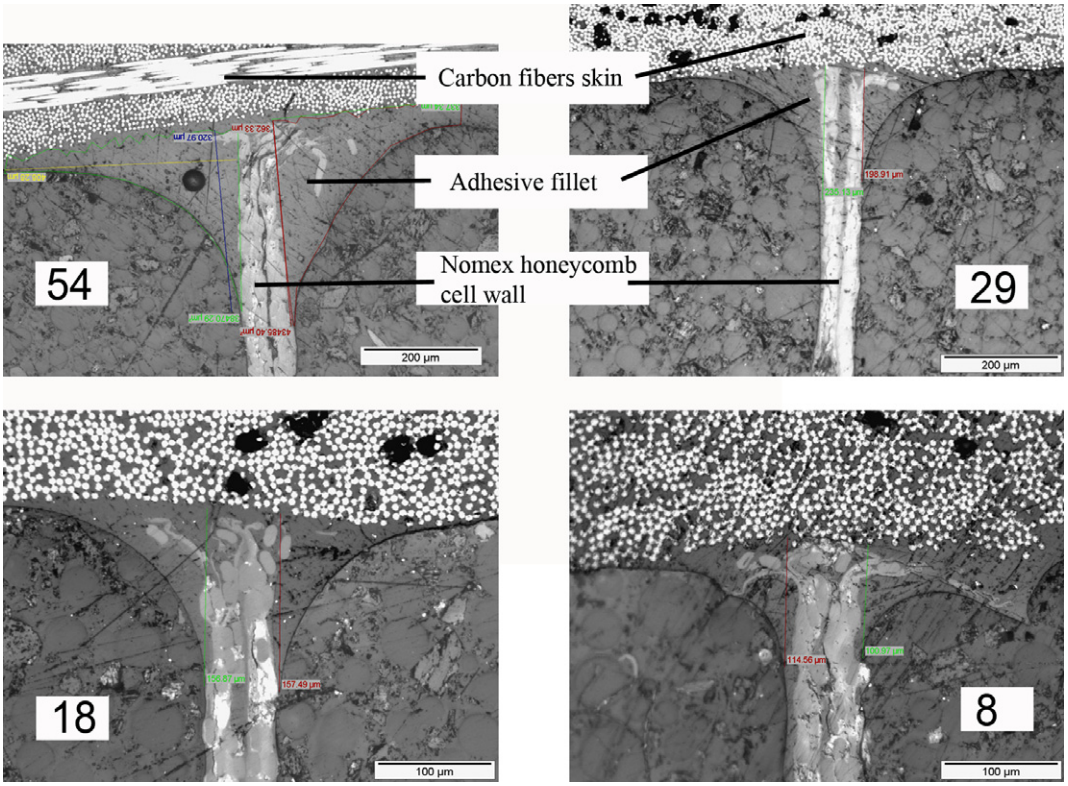

Fig. 12. Resin fillet with 54, 29, 18 and 8 g/m^2 adhesive. The size increases with adhesive weight. The end of the honeycomb cell walls is crushed, and this distorts the shape of the meniscus, especially at low adhesive weight. Note that the scale is different on the two lower micrographs.

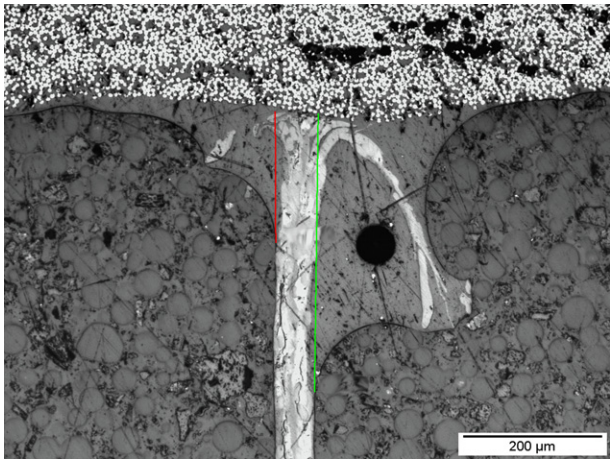

Fig. 13. Adhesive meniscus forming between honeycomb cell wall and carbon fiber skin, with 25 g/m^2 adhesive. Aramid fibers from the Nomex honeycomb cell wall completely change the shape of the meniscus. An air bubble due to resin degassing is also visible.

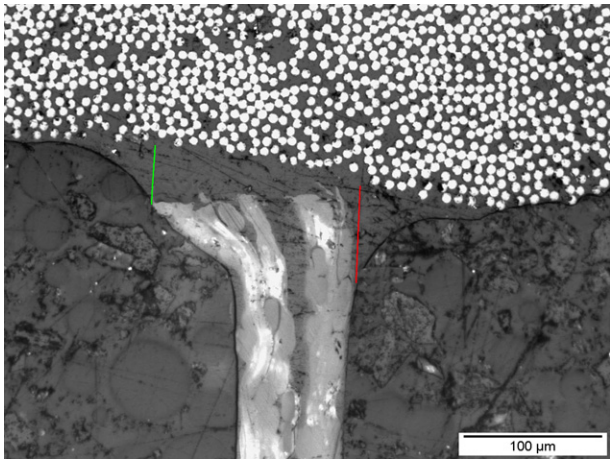

Fig. 14. Adhesive meniscus forming between honeycomb cell wall and carbon fiber skin, with 12 g/m^2 adhesive. Some of the adhesive is in the resin meniscus, but some remains between the cell wall and the prepreg.

in the meniscus was then set to 25 g/m^2 in the model which, in this case, predicted very well the size of the meniscus (Fig. 16).

It was also interesting to observe that in the case of a 50 g/m^2 adhesive film on already cured prepreg, half of the resin was not

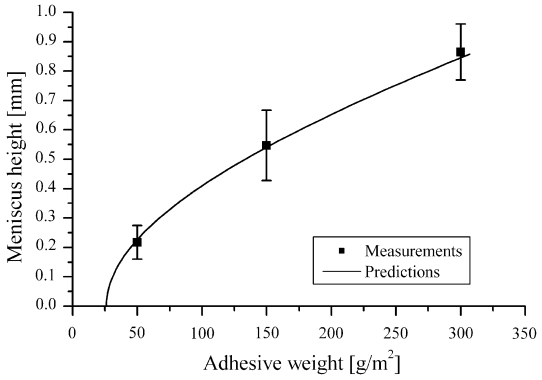

Fig. 16. Meniscus height predicted as a function of adhesive weight and contact angles. The contact angle with the carbon was considered as 0° and with the Nomex as 14°. The corresponding shape factor is $\alpha = 0.52$. The adhesive weight M_0 which is not in the meniscus is considered as 26 g/m^2.

used to bond the core to the skin and merely constituted additional weight. This shows the advantage of the resin deposition method when small quantities of adhesive are used. Another alternative is to use one-shot curing of the sandwich panel, so that part of the prepreg resin can be used to form the meniscus. However this method has the clear disadvantage of producing skin of reduced quality, especially when thin skins are used. In fact the skin compacted under the core only has pressure under the honeycomb cell wall, and not in the center of the cell, where large voids can then be found between the laminas. The skin cured on top of the honeycomb will present the well known telegraphic effect [38] because of the skin penetrating into the honeycomb cells, thus reducing the strength and stiffness of the skin. The adhesive deposition method associated with the meniscus size prediction model is thus a really appropriate method for producing high quality ultra-light sandwich panels.

5. Conclusions

Bonding between a honeycomb core and CFRP skins was studied with particular emphasis on meniscus formation between the honeycomb cell walls and the skins. A method was developed allowing the quantity of adhesive used for core-to-skin bonding to be tailored, thus making it possible to study the size and shape of the meniscus with controlled adhesive quantities as low as 8 g/m^2 and up to 80 g/m^2.

To predict the shape of the adhesive meniscus, the contact angles between the adhesive and the Nomex and carbon skin were measured. A very pronounced contact angle hysteresis, due to high adhesive viscosity and rough surfaces, was highlighted.

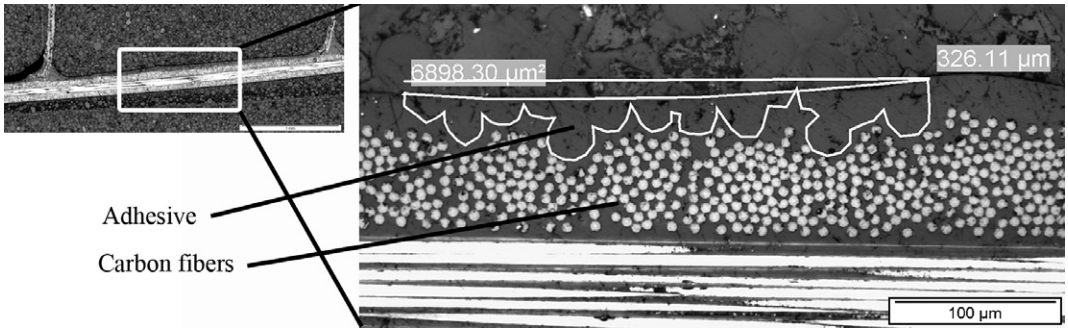

Fig. 15. Measurement of the mean thickness of adhesive left on the surface of the prepreg by adhesive film. The area delimited by the white contour is adhesive on top of the rough prepreg surface. The mean thickness, calculated by dividing the area by the length of the zone considered, was 21 µm in the present case, which represents 25 g/m^2 adhesive.

A model was developed to predict the shape and size of the meniscus on the basis of the contact angles. It was shown that the meniscus surface adopts a circular shape at equilibrium when the menisci are small enough to be unaffected by gravity. This was confirmed on the micrographs of sandwich panels' cross-sections.

The model predicting the height of the meniscus showed very good agreement with the measurements on sandwich cross-sections, providing the residual layer of adhesive on the skin surface is taken into account. Prediction of adhesive fillet size and geometry can be used as first step in predicting the microscopic failure mechanisms [39], and thus the bonding quality between honeycomb core and skin and its influence on sandwich panels' strength [40].

Acknowledgements

The authors wish to acknowledge the EPFL and the Swiss Innovation Promotion Agency (CTI, #8002.1, DCPP-NM) for financial support.

References

[1] Funke H. Systematische Entwicklung von Ultra-Leichtbaukonstruktionen in Faserverbund-Wabensandwichbauweise am Beispiel eines Kleinflugzeuges. Ph.D. Dissertation, Universität-GH Paderborn, Germany, 2001.
[2] Funke H. Development of the ultralight aircraft silence. JEC – Composites 2004;10:52–4.
[3] Middleton DH. Composite materials in aircraft structures. Harlow: Longman; 1990.
[4] Rozant O, Bourban PE, Månson JAE. Manufacturing of three dimensional sandwich parts by direct thermoforming. Compos Part A – Appl Sci Manuf 2001;32(11):1593–601.
[5] Triantafillou TC, Gibson LJ. Minimum weight design of foam core sandwich panels for a given strength. Mater Sci Eng 1987;95:55–62.
[6] Triantafillou TC, Gibson LJ. Failure mode maps for foam core sandwich beams. Mater Sci Eng 1987;95:37–53.
[7] Daniel IM, Abot JL. Fabrication, testing and analysis of composite sandwich beams. Compos Sci Technol 2000;60(12–13):2455–63.
[8] Gibson LJ, Ashby MF. Cellular solids, structure and properties. Cambridge: Cambridge University press; 1988.
[9] Zenkert D. The handbook of sandwich construction. Cradley Heath: EMAS; 1997.
[10] Ley RP, Lin W, Mbanefo U. Facesheet wrinkling in sandwich construction. NASA/CR-199-208994, Langley Research Center, Hampton, Virginia, 1999.
[11] Thomsen OT, Banks WM. An improved model for the prediction of intra-cell buckling in CFRP sandwich panels under in-plane compressive loading. Compos Struct 2004;65(3–4):259–68.
[12] Fagerberg L, Zenkert D. Imperfection-induced wrinkling material failure in sandwich panels. J Sandw Struct Mater 2005;7(3):195–219.
[13] ASTM C 297-94, standard test method for flatwise tensile strength of sandwich constructions. Annual Book of ASTM Standards, 1994, 15.03.
[14] ASTM D 5528-94a, standard test method for mode 1 interlaminar fracture toughness of unidirectional fiber-reinforced polymer matrix composites. Annual Book of ASTM Standards, 1994, 15.03.
[15] ASTM D 1781-98, standard test method for climbing drum peel for adhesives. Annual Book of ASTM Standards, 1998, 15.06.
[16] Avery JL, Sankar BV. Compressive failure of sandwich beams with debonded face-sheets. J Compos Mater 2000;34(14):1176–99.
[17] Cantwell WJ, Davies P. A test technique for assessing core skin adhesion in composite sandwich structures. J Mater Sci Lett 1994;13(3):203–5.
[18] Cantwell WJ, Davies P. A study of skin-core adhesion in glass fibre reinforced sandwich materials. Appl Compos Mater 1996;3(6):407–20.
[19] Cantwell WJ, Scudamore R, Ratcliffe J, Davies P. Interfacial fracture in sandwich laminates. Compos Sci Technol 1999;59(14):2079–85.
[20] Ratcliffe J, Cantwell WJ. A new test geometry for characterizing skin-core adhesion in thin-skinned sandwich structures. J Mater Sci Lett 2000;19(15):1365–7.
[21] Okada R, Kortschot MT. The role of the resin fillet in the delamination of honeycomb sandwich structures. Compos Sci Technol 2002;62(14):1811–9.
[22] Grove SM, Popham E, Miles ME. An investigation of the skin/core bond in honeycomb sandwich structures using statistical experimentation techniques. Compos Part A – Appl Sci Manuf 2006;37(5):804–12.
[23] G, Lecci U, Marchetti M, Poscente F. Fem simulation of the mechanical behaviour of sandwich materials for aerospace structures. In: Experimental techniques and design in composite materials, vol. 5, 2002. p. 209–20..
[24] Rion J, Geiser A, Leterrier Y, Månson J-AE. Ultralight composite sandwich structure: optimization of skin to honeycomb core bonding. In: Proceedings of 27th International Conference of SAMPE Europe, Paris, 2006.
[25] Hayes BS, Seferis JC, Edwards RR. Self-adhesive honeycomb prepreg systems for secondary structural applications. Polym Composite 1998;19(1):54–64.
[26] Chanteranne J. Use of ultra-light adhesive for the metal-honeycomb bonding. Ann Chim – Sci Mat 1987;12(2):199–204.
[27] Benard Q, Fois M, Grisel M. Peel ply surface treatment for composite assemblies: chemistry and morphology effects. Compos Part A – Appl Sci Manuf 2005;36(11):1562–8.
[28] Adamson AW, Gast AP. Physical chemistry of surfaces. New-YorkNew York: John Wiley & Sons; 1997.
[29] Kinloch AJ. Adhesion and adhesives: science and technology. London: Chapman and Hall; 1987.
[30] Packham DE. Handbook of adhesion. Chichester: John Wiley & Sons; 2005.
[31] Wenzel RN. Resistance of solid surfaces to wetting by water. Ind Eng Chem 1936;28:988–94.
[32] Wenzel RN. Surface roughness and contact angle. J Phys Colloid Chem 1949;53(9):1466–7.
[33] Wolansky G, Marmur A. Apparent contact angles on rough surfaces: the Wenzel equation revisited. Colloid Surface A 1999;156(1–3):381–8.
[34] Benard Q, Fois M, Grisel M. Roughness and fibre reinforcement effect onto wettability of composite surfaces. Appl Surf Sci 2007;253(10):4753–8.
[35] Page SA, Mezzenga R, Boogh L, Berg JC, Månson J-AE. Surface energetics evolution during processing of epoxy resins. J Colloid Interf Sci 2000;222(1):55–62.
[36] Smith PG, Van De Ven TGM. Profiles of slightly deformed axisymmetric drops. J Colloid Interf Sci 1984;97(1):1–8.
[37] Orr FM, Scriven LE, Rivas AP. Pendular rings between solids – meniscus properties and capillary force. J Fluid Mech 1975;67(25):723–42.
[38] Altstadt V, Diedrichs F, Lenz T, Bardenhagen H, Jarnot D. Polymer foams as core materials in sandwich laminates (comparison with honeycomb). Polym Polym Compos 1998;6(5):295–304.
[39] Rion J, Demarco F, Leterrier Y, Månson J-AE. Damage analysis of ultralight sandwich structures. In: Proceedings of 16th International Conference on Composite Materials, Kyoto, 2007.
[40] Rion J, Stutz S, Leterrier Y, Månson J-AE. Influence of process pressure on local facesheet instability for ultralight sandwich structures. In: Proceedings of Eighth International Conference on Sandwich Structures, Porto, 2008.